

TITLE OF THE INVENTION ANISOTROPY BASED SENSING

5

CROSS-REFERENCES TO RELATED APPLICATIONS

This application claims the benefit of application

Serial No. 60/107,997 filed November 11, 1998.

10

15

STATEMENT REGARDING FEDERALLY SPONSORED RESEARCH OR DEVELOPMENT

The work described herein was supported by a grant from the National Institutes of Health National Center for Research Resources RR-08119 and RR-10955.

BACKGROUND OF THE INVENTION

- 1. Field of the Invention
- The present invention relates to the determination of the presence or concentration of an analyte in a sample, using anisotropy based sensing techniques employing fluorescent sensing and reference molecules.
- 25 2. Description of the Related Art

A bibliography follows at the end of the Detailed Description of the Invention. The listed references are all incorporated herein by reference.

The technology for chemical sensing using

fluorescence is advancing rapidly due to the continued introduction of new concepts, new fluorophores and proteins engineered for sensing specific analytes [1-7]. New approaches to chemical sensing include lifetime-based sensing [8-10] and the use of metal-ligand complexes with

microsecond decay times [11-12]. Recently there has been

5

10

15

20

25

30

an increased interest in the use of reference fluorophores as part of the sensor design. idea is to mix the sensing fluorophore with another fluorophore which is not sensitive to the analyte. combined emission from both species is used to determine the concentration of the analyte. This approach has been used with a long lifetime reference and phase angle measurements to develop sensors for pH and pCO2 [13-14]. The present inventors have used such mixtures with modulation measurements for chemical sensing [15-17]. When the sensor contains a mixture of a fluorophores with nanosecond and microsecond decay times the modulation of the emission, at appropriate low frequencies, becomes equal to the fractional intensity of the nanosecond fluorophore. This approach was used to develop sensors for glucose, pH and calcium [15-17].

However, there remains a need in the art for improved methods for determining the presence or concentration of an analyte using fluorescent reference and sensing molecules.

BRIEF SUMMARY OF THE INVENTION

In one aspect, the present invention relates to a method for determining the presence or concentration of an analyte, comprising the steps of:

- a) exposing a fluorescent reference molecule and a fluorescent sensing molecule to a radiation source;
- b) measuring a first level of anisotropy of the fluorescence emitted by said molecules;
 - c) exposing said sensing molecule to an analyte, wherein said analyte is capable of changing the intensity of the fluorescence emitted by the sensing molecule;
- d) measuring a second level of anisotropy of the
 35 fluorescence emitted by said molecules after exposure of

10

25

30

35

the sensing molecule to said analyte; and

e) correlating a change in said second level of anisotropy with the presence or concentration of said analyte.

In another aspect, the present invention relates to a device for determining the presence or concentration of an analyte in a sample, which comprises:

- a) means for exposing a fluorescent reference molecule and a fluorescent sensing molecule to a radiation source;
- b) means for measuring the anisotropy of the combined fluorescence emitted by said molecules;
- c) means for exposing said sensing molecule to an analyte;
- d) optionally means for correlating a change in said level of anisotropy from before to after exposure to the analyte with the presence or concentration of said analyte; and
- e) optionally a radiation source capable of causing
 20 said reference and sensing molecules to emit fluorescence.

BRIEF DESCRIPTION OF THE DRAWINGS

Figure 1 shows the emission spectra of erythrosin B in water at 20°C , in the presence of the $[\text{Ru}(\text{bpy})_3]^{2+}$ reference. The dashed line shows the transmission of the emission filter used for the anisotropy measurements.

Figure 2 shows the concentration dependence of the steady state anisotropy of ErB, in the absence (0) and presence (\bullet) of the $[Ru(bpy)_3]^{2+}$ reference. Anisotropies were measured using the emission filter shown in Figure 1 (---).

Figure 3 shows the absorption and emission spectra of pyridine 2 in a polyvinyl alcohol film. Also shown are the excitation (---) and emission $(\cdot \cdot \cdot \cdot)$ anisotropy

spectra.

5

10

20

25

30

35

Figure 4 shows fluorescence anisotropy as a function of stretching for Py2 in PVA film. R_s is the stretching ratio, $R_s = N^{3/2}$ where N is the fold of the stretch [23].

Figure 5 shows the emission spectra of the high anisotropy PVA film in the presence of 6-carboxy fluorescein at various pH values.

Figure 6 shows a plot of anisotropy versus pH for a pH sensor based on 6-carboxy fluorescein and Py2-PVA film.

Figure 7 shows the emission spectra of the Py2-PVA film in the presence of increasing concentrations of $[Ru(bpy)_3]^{2+}$.

Figure 8 shows the steady state anisotropy of the Py2-PVA- $[Ru(bpy)_3]^{2+}$ sensor with increasing concentrations of $[Ru(bpy)_3]^{2+}$.

Figure 9A shows the emission spectra of Py2-PVA film with increasing concentrations of Ru-HSA. Figure 9B shows the emission spectra with different concentrations of Py2 in the film, and the same concentration of Ru-HSA.

Figure 10 shows the steady state anisotropy of Py2-PVA film with increasing concentrations of Ru-HSA.

Figures 11(A-C) are schematics of anisotropy sensors with a zero anisotropy (11A) or high anisotropy reference (11B and 11C). When using an oriented film as the reference, excitation can be performed without a polarizer (11C).

Figure 12 is a schematic of a polarization based sensor with a self-referenced sample.

Figure 13 depicts a polarization-based oxygen sensor.

Figure 14A shows the emission spectra from the combined oxygen sensor shown in Figure 13 observed with the analyzer polarizer in the vertical (V) or horizontal (H) orientation. The dotted lines show the emission

5

10

15

20

25

30

35

spectra of the $Ru(dpp)_3Cl_2$ film alone as seen through the horizontal analyzer. Figure 14B shows the wavelength-dependent polarization of the combined emission from the oxygen sensor.

Figure 15 shows a plot of polarization versus oxygen concentration.

Figures 16A and 16B show the emission spectra of the vertical (V) and horizontal (H) components from the combined sensor. The vertical polarizer is placed in front of the ANS/HSA solution. The horizontal polarizer is placed in front of the ANS-Q26C GGBP sample. The upper and lower panels show the component spectra in the absence and presence of 8 μ M glucose, respectively.

Figure 17 shows the wavelength-dependent polarization of the combined emission from ANS-Q26c GGBP and ANS/HSA. The arrow shows the wavelength chosen for measurement of the glucose concentration.

Figure 18 shows the glucose-dependent polarization values from the two-part sensor.

Figure 19 shows the emission spectra (19A) and polarization spectra (19B) for a two-part sensor consisting of only ANS-Q26C GGBP in both sides of the sensor. The glucose concentration was constant on the left (V) side of the sensor, and was varied in the right (H) side of the sensor (see Figure 12).

Figure 20 shows glucose-dependent polarization sensing using only ANS-Q26C GGBP in both sides of the sensor.

Figure 21 shows polarization sensing of calcium using Fluo-3. Figure 21A shows the emission spectra of the vertical component (Figure 12, R) and of the horizontal component (Figure 12, S). The calcium concentration is constant at 1,35 μ M in the left side (R) of the sensor. The calcium concentration is variable in the right side of the sensor (S). Figure 21B shows the

10

15

20

25

30

35



polarization across the emission spectra.

Figure 22 shows calcium-dependent polarization values using only Fluo-3 in both sides of the sensor.

Figure 23 Shows the luminescence spectra of the oxygen probe $Ru(dpp)_3Cl_2$ in silicon, in the presence of nitroge;, air and oxygen.

Figure 24 shows the luminescence intensity of the oxygen-sensitive film of $Ru(dpp)_3Cl_2$ in silicon upon repeated exposure to nitrogen and air.

Figure 25 shows the absorption (A), emission (F) and polarization spectra $(---, \cdots)$ of reference Styryl 7 in the unoriented PVA film.

Figure 26 shows the fluorescence polarization of Styryl 7 in the PVA film as a function of the stretching ratio $R_s=N^{3/2}$, where N is the physical fold of the stretch.

DETAILED DESCRIPTION OF THE INVENTION

The present invention relates to a different approach to sensing based on the use of reference fluorophores. This new method is based on the anisotropy of the reference, rather than its decay time. The sensor is designed so that one observes emission from both the sensing fluorophore and a reference fluorophore. reference fluorophore can display an anisotropy near zero (for example, below about 0.2), or can be near unity (for example, above about 0.6) for fluorophores embedded in oriented films. The only requirements for sensing are that the sensing fluorophore change concentration or intensity in response to the presence of the analyte, and that it displays an anisotropy different from the reference. Under these conditions the analyte concentrations can be determined from a simple measurement of the steady state anisotropy of the combined emission from the reference and sensor

molecules.

5

25

The theory for anisotropy sensing is simple, and is based on the additivity property of anisotropies demonstrated by Jabłoński [18]. Suppose one observes the steady state emission from two species, the sensing fluorophore which is sensitive to the analyte (S) and the reference fluorophore which is not sensitive to analyte (R). The measured anisotropy (r) is given by the intensity-weighted average of the individual anisotropies

$$r = r_s f_s + r_R f_R. \tag{1}$$

In this expression f_s and f_R are the fractional intensities of the two species, f_s + f_R = 1.0. The intensity and anisotropy of the reference fluorophore is independent of the analyte. Any factor which results in a changing intensity of the sensing fluorophore will result in a change in the measured anisotropy. Hence this approach to sensing can be used to detect the presence of any analyte which causes a change in intensity of the sensing fluorophore. A large number of fluorophores are known to change intensity in response to cations, anions and various other analytes [5, 10].

The advantage of anisotropy sensing can be seen by considering an anisotropy assay based on protein-protein interactions. Suppose a fluorophore with a lifetime $\tau=10$ ns is bound to a protein with a rotational correlation time $\theta=5$ ns, and that the fluorophore is rigidly bound to the protein. Assuming the fundamental anisotropy $r_0=0.4$, the steady state anisotropy of the labeled protein is given by the Perrin equation,

$$r = \frac{r_0}{1 + \tau/\Theta} \tag{2}$$

30 which in this case is equal to 0.133. Now suppose the

5

10

15

20

25

30

35

labeled protein binds to a larger protein such that the correlation time increases to 40 ns. The steady state anisotropy will then increase to r=0.32. The total anisotropy change will thus be 0.19. The actual changes in anisotropy are often smaller than 0.19 due to r_0 values less than 0.4 and segmental motion of the fluorophore on the protein.

An anisotropy assay using a reference fluorophore can have a much wider range of anisotropy values. This is because the reference fluorophore can be chosen to have an anisotropy near zero or near one. Anisotropies near zero are easily obtained for fluorophores with nanosecond lifetimes in aqueous solutions. Correlation times for fluorophores in water are near 100 ps, so any lifetime above 1 ns results in nearly complete depolarization. Also, the luminescent metal ligand complex have lifetimes of hundreds of ns to several microseconds [19-20], and thus display anisotropies of zero when dissolved in water.

In addition to a zero anisotropy reference, one can also easily obtain a reference signal with an anisotropy near unity. For example, such values can be obtained for fluorophores in stretched polymer films, which result in elongated fluorophores being aligned along the stretching axis [21]. In such systems the electronic transitions of the fluorophore are all aligned in one direction, or more precisely, display a uniaxial orientation. The emission anisotropy from such samples are typically in the range of 0.6 to 0.8, and can approach 1.0 [22-23]. polymer films are easy to prepare and retain their orientation for extended periods of time. fluorophores randomly distributed in solution the maxima observed value of the anisotropy is 0.4 with single photon excitation. The lowest possible value for randomly oriented fluorophores is -0.2. In general for

0983 35 072001 PCT/US99/26480

WO 00/28327

5

10

15

20

25

30

35

polarization assays to measure association reactions of biological macromolecules, the typical range is less than 0.2 anisotropy units. Hence, the use of a reference fluorophore and anisotropy sensing can expand the dynamic range of anisotropy values from 0.0 to 1.0, as compared with a typical range of less than 0.2 anisotropy units.

One advantage of anisotropy-based sensing according to the present invention is that anisotropy measurements are intrinsically ratiometric, and provide an absolute value which can be readily compared between instruments. A further advantage is that any sensing fluorophore which changes intensity can be used with the present invention, thus changing an intensity measurement to a ratiometric anisotropy measurement. The use of a reference fluorophore expands the dynamic range of the anisotropy to almost two full units, -1.0 to 1.0. While most of the results in the present application are presented in terms of the anisotropy, calculation of the anisotropy is not required. For an analytical or clinical application the ratio I_1/I_1 can be used directly for the calibration curve.

It will be appreciated that in practice of the present invention, the analyte calibration curve will depend on the concentrations of the sensing and reference fluorophores, and on the excitation and emission wavelengths. Thus, it may be desirable to maintain a substantially constant concentration of the fluorophores by, for example, covalently linking the fluorophores to each other, or to the supporting matrices.

Anisotropy-based sensing provides a valuable method for clinical chemistry, where the measurements must be accomplished with high accuracy and with simple and/or portable instruments.

According to the present invention, any sensing fluorophore which displays a change in intensity can be

5

10

15

20

25

30

35

used to create an anisotropy-based sensor. Fluorophores displaying intensity changes are known for a wide variety of ions, including sodium, potassium, calcium, magnesium, zinc, chloride, phosphate, and oxygen [10, 34-44], as well as for measurement of pH. In addition, the present invention may be used to detect the presence or concentration of all sorts of other biochemicals having physiological significance, including proteins, lipoproteins, glycoproteins, peptides, nucleic acids, polysaccharides, lipopolysaccharides, lipids, fatty acids, cellular metabolites, hormones, pharmacological agents, antibodies, sugars (such as glucose), etc.

Additionally, film-type sensors which contain the high anisotropy reference and an immobilized sensing fluorophore are preferable in many applications. The anisotropy of such sheet-type sensors may be used for determination of ion concentrations in a wide variety of situations.

The fluorescent reference molecule is chosen to provide a constant reference or background. There are a wide range of commercially available suitable reference molecules, for example those sold by Molecular Probes, Inc., Eugene, Oregon and other companies.

In one embodiment of the present invention, the reference molecule may have the same structure as the sensing molecule, in which case the reference molecule is not exposed to the analyte, e.g., is isolated in a separate compartment or the like. When the reference and sensing molecules have different structures, the reference molecule may be exposed to the analyte provided that such exposure does not change the intensity of the fluorescence emitted by the reference molecule. If such exposure would change the intensity, then the reference molecule should remain isolated from the analyte.

The present invention will be further illustrated by

means of the following non-limiting examples. In the examples, the following abbreviations are used:

ErB erythrosin B

Py2 pyridine 2 [1-ethyl-4-(4-(p-

5 dimethylaminophenyl)-1,3-butadienyl)-pyridinium

perchloratel

PVA polyvinyl alcohol

6-CF 6-carboxy fluorescein

HSA human serum albumin

10 bpy 2,2'-bipyridyl

20

25

30

phen-IA 5-iodoacetamido-1,10-phenanthroline

Ru-HSA HSA covalently labeled with [Ru(bpy), (phen-

 $IA)](PF_6)_2$

LED light emitting diode

15 MLC metal-ligand complex

anisotropy is given by

ANS 8-anilino-1-naphthalenesulfonic acid

The experiments described in Examples 1-5 were performed using sensors configured as shown in Figure 11. Excitation was with the 514 nm output of an air-cooled argon ion laser, or with a blue LED from Nichia Chemical Industries, Tokushima, Japan. When using an LED an excitation bandpass of 466 ± 26 nm was selected [24] using a 510 nm short wavepass filter. The laser excitation was vertically polarized, and the emission observed through a polarizer oriented parallel (||) or perpendicular (1) to the electric vector of the excitation. For experiments with the LED excitation source we did not use an excitation polarizer. using an oriented film there is no need to use an excitation polarizer because the emission is highly polarized with polarized or unpolarized excitation. The

$$r = \frac{I_{\parallel} - GI_{\perp}}{I_{\parallel} + 2GI_{\perp}} \tag{3}$$

10

15

20

25

30

where I_{i} and I_{i} are the intensities observed with emission polarizer parallel or perpendicular to the polarized excitation, respectively. The G factor is the ratio of intensities (I_{i}/I_{i}) observed with horizontally polarized excitation [25]. In our apparatus the G-factor was near 1.0. For experiments without an excitation polarizer we used the G-factor measured with an excitation polarizer. This is acceptable because the G-factor is a property of the detection system, and not dependent on the method of excitation.

EXAMPLE 1

Erythrosin B was obtained from BDH, $[Ru(bpy)_3]^{2+}$ was obtained from GFS Chemicals, and 6-carboxy fluorescein from Eastman Kodak, and used without further purification. Pyridine 2 was obtained from Exciton, Inc. Films of polyvinyl alcohol were prepared as described previously [22-23]. These films were stretched up to 6-fold to orient the Py2 molecules and the film was then pressed against the side of the cuvette (Figure 11). When using stretched films the stretching ratio (R_s) is defined as the axial ratio a/b of an ellipse which is formed when stretching an imaginary circle in the unoriented film [23]. The volume of the circle on ellipse is assumed to be conserved. Under these conditions

$$R_S = N^{3/2} \tag{4}$$

where N is the physical fold of the stretch.

The sulfhydryl reactive ruthenium metal-ligand complex $[Ru(bpy)_2(phen-IA)](PF_6)_2$ was prepared as described previously [26]. Human serum albumin was labeled using a 5-fold molar excess of this complex in phosphate buffer, pH 7.1 overnight at 4°C. Unreacted dye was removed with a Sephadex G-15 column, followed by

5

10

15

20

25

30

35

dialysis overnight against phosphate buffered saline. The dye-to-protein molar ratio was near 0.40, as determined using the molar extinction coefficient for HSA of $3.7 \times 10^4 \,\mathrm{M}^{-1} \,\mathrm{cm}^{-1}$ at 280 nm and 64,500 and 16,600 $\mathrm{M}^{-1} \,\mathrm{cm}^{-1}$ for the ruthenium complex at 280 and 450 nm, respectively. However, only labeled protein is observed in this experiment, so the effective dye-to-protein ratio is near 1.0.

The concept of anisotropy sensing was tested using a mixture of fluorophores. We chose [Ru(bpy)₃]²⁺ as the reference. The decay time of this complex in water is near 400 ns, and its steady state anisotropy is essentially zero, independent of the excitation wavelength. To model a sensing fluorophore with a nonzero anisotropy we chose erythrosin B. In water at 20°C this fluorophore displays a decay time of 75 ps [27]. The short lifetime is expected to result in a nonzero anisotropy. Erythrosin B was also chosen because it could be excited with the same 514 nm laser, and displays a high fundamental anisotropy r₀ near 0.4 at this wavelength [27].

Emission spectra of the ErB-[Ru(bpy)₃]²⁻ mixture are shown in Figure 1. The emission centered at 550 nm is due to ErB, and increases as the ErB concentration increases. The shoulder at 620 nm is due to $[Ru(bpy)_3]^{2+}$, which is present at the same concentration for all these emission spectra. For anisotropy sensing the combined emission of ErB and $[Ru(bpy)_3]^{2+}$ was observed through a filter whose transmission is shown in Figure 1 (---). This filter attenuated the emission at ErB relative to that of the reference so that both fluorophores made comparable contributions to the detected emission.

Steady state anisotropies for this sensor are shown in Figure 2. For ErB alone, without $[Ru(bpy)_3]^{2+}$, the anisotropy is independent of the ErB concentration (O),

and displays a constant value of 0.18. For the mixture the anisotropy is strongly dependent on the ErB concentration. At low ErB concentrations the anisotropy is near zero because the $[Ru(bpy)_3]^{2+}$ has an anisotropy near zero. The anisotropy increased dramatically as the ErB concentration increases relative to that of $[Ru(bpy)_3]^{2+}$.

The data for the ErB - [Ru(bpy)₃]²⁺ mixture are presented in Table I, along with comparison of expected and calculated fractional intensities. The anisotropy of the mixture was used to calculate the fractional intensity of ErB. These calculated values are in excellent agreement with the fractional intensities found from the intensity measurements on the control samples containing a single fluorophore. These results (Figure 1 and Table I) demonstrate that anisotropy sensing can be used with any sensing fluorophore which displays an intensity change in response to analyte and a non-zero anisotropy.

20

5

10

15

	<u>Table I</u>					
	[ErB]	[Ru (bpy) 3] 2+	I, a	f _{ErB} b	r	fers calc, c
	(Mu)	(µM)				
	0	20	1275	0	0	0
5	0.5	20	1720	0.258	0.043	0.237
	1	20	2250	0.433	0.075	0.414
	2	20	3234	0.606	0.109	0.602
	3	20	4081	0.687	0.122	0.674
	4	20	5080	0.749	0.138	0.762
10	5	20	6035	0.789	0.144	0.796
	6	20	7040	0.819	0.147	0.812
	7	20	7705	0.834	0.149	0.823
	8	20	8570	0.851	0.153	0.845

^aTotal fluorescence intensity, $I_T = I_1 + 2I_1$.

^c Fractional intensity of ErB calculated from the anisotropy data. This value was calculated using $f_{\text{ErB}}^{\text{calc}} = r/r_s$ where r_s in the anisotropy of ErB in the absence of $[\text{Ru}(\text{bpy})_3]^{2+}$.

EXAMPLE 2

25 Another approach to anisotropy based sensing makes use of the high anisotropy values available from oriented systems. Oriented samples can be easily prepared by the use of stretched polymer films [21-23]. We chose the laser dye pyridine 2 (Py2) because of its favorable spectral properties. Absorption and emission spectra of Py2 in a PVA film are shown in Figure 3. Py2 can be excited at 514 nm and displays a reasonable Stokes' shift. Importantly, Py2 displays a high fundamental anisotropy which is mostly independent of the excitation and emission wavelengths.

The anisotropy of Py2 in the PVA film can be increased dramatically by mechanical stretching. As the

^b Fractional intensity of ErB. This value was calculated using $f_{\text{ErB}} = (I - I_{\text{R}})/I$, where I_{R} is the intensity of the $[\text{Ru}(\text{bpy})_3]^{2+}$ in the absence of ErB.

10

15

20

25

30

35

stretching ratio is increased the anisotropy increases from 0.34 for the unoriented film to nearly 0.9 for a film which has been stretched 5- to 6-fold (Figure 4). The use of a stretched film can eliminate the need for an excitation polarizer and thus decrease the cost and complexity of the instrument. This is shown by comparing the anisotropy values for the Py2-PVA film observed with polarized and unpolarized excitation (Figure 4). more precise, we mimicked unpolarized excitation with a beam rotator, so that the electric vector of the excitation was 45° from the vertical orientation. the unstretched film the anisotropy with 45° excitation is one-half of that found for vertically polarized excitation, which agrees that the values expected for the theory of anisotropy [25].

It is important to notice the dependence of the anisotropies as the PVA film is stretched, with polarized and unpolarized excitation. For unpolarized excitation the anisotropy increases more rapidly with stretching than for polarized excitation (Figure 4). At high stretching ratios the anisotropies are nearly equal independent of whether the excitation is polarized on unpolarized. This occurs because the electronic transitions are oriented along these vertical axis. Hence the emission is polarized along this axis even if the excitation is unpolarized or polarized at 45° from the vertical. Hence, the oriented film serves the same purpose of an excitation polarizer and results in alignment of the electronic transitions with this vertical axis.

EXAMPLE 3

As an additional example of anisotropy sensing we chose to develop a pH sensor using the oriented film as a

5

10

15

20

25

30

35



reference. We chose 6-carboxy fluorescein as a pH sensitive fluorophore. Fluorescein has been widely used for pH sensing [28-30]. Fluorescein and its derivatives display a pH-dependent dissociation of the carboxy group. The ionized form which exists at pH values above 7.5 is highly fluorescent, and the protonated low pH form is essentially non-fluorescent. Hence, the intensity of fluorescein increases over the pH range from 5 to 7.

Since fluorescein displays a lifetime near 4 ns, its anisotropy in water is expected to be near zero. Hence, we could not use the zero anisotropy reference [Ru(bpy)₃]²⁺. We used the high anisotropy reference, pyridine 2 (Py2) in a stretched PVA film. For these experiments the PVA film stretched 5.5-fold and displayed anisotropy near 0.9. This value is above the usual theoretical limit of 0.4 because this latter value applies to randomly distributed fluorophores.

Emission spectra of the Py2-6-CF pH sensor are shown in Figure 5. The same fluorescein concentration is present for all spectra, but the pH is varied. As the pH increases so does the intensity of the fluorescein relative to that of the Py2-PVA reference. Anisotropies are shown in Figure 6. As the pH increases the anisotropy decreases. At low pH the anisotropies exceed 0.4 because of the high anisotropy from the Py2-PVA film. Anisotropy measurements are readily accurate to ± 0.002. For this degree of accuracy, the pH is expected to be accurate to ± 0.02, which is adequate for clinical measurement of pH as done for blood gas determination [31-33].

EXAMPLE 4

Binding of proteins to surfaces is used in a wide variety of biomedical assays [45]. Hence we considered how anisotropy-based sensing could be used to detect the

10

15

20

30

35

WO 00/28327

presence of labeled proteins near surfaces. This situation was modeled using the stretched film and a long lifetime metal-ligand complex ("MLC") in water. selected this model system because there has been significant progress in the design and synthesis of conjugatable MLCs with long lifetimes in aqueous solution [11, 46-47]. While the emission of MLC-labeled proteins is usually polarized, the anisotropies are often low. Hence the most promising approach appears to be the decrease in anisotropy expected from the combined emission of a MLC and the Py2-PVA film. experiment we used front-face geometry (Figure 11B).

To test this concept we examined the Py2-PVA film in the presence of increasing amounts of $[Ru(bpy)_3]^{2+}$. Emission spectra for the Py2-PVA film and [Ru(bpy)3]2+ are shown in Figure 7. In this case the emission spectra overlap strongly, and one cannot easily identify the two species in the spectra. The intensity of the emission at 600 nm increases as the [Ru(bpy)₃]²⁺ concentration increases. The anisotropy decreases rapidly as the [Ru(bpy)₃]²⁺ concentration increases (Figure 8). anisotropies seem to be particularly sensitive to low concentrations of the Ru complex.

25 EXAMPLE 5

> Anisotropy sensing is a useful way to detect protein binding to surfaces. For instance, Py2-PVA surface may contain antibodies for a desired antigen, and the assay mixture may include a Ru-labeled antigen. In such a case the concentration of Ru-labeled protein near the surface would depend on the antigen concentration in the sample, as is typical in a competitive assay. We tested the feasibility of such a sensor using human serum albumin (HSA) labeled with [Ru(bpy), (phen-IA)]2+ (Figure 9). this case we varied the concentration of Py2 in the PVA

0983 35 072001 PCT/US99/26480

WO 00/28327

5

10

15

20

25

(bottom) film as well as the bulk concentration of Rulabeled HSA (Ru-HSA) (top). These measurements were done using the in-line geometry (Figure 11C), which is comparable to a front face measurement. For these cases the anisotropy from an isotropic sample is always zero, even if non-zero for right angle observation. However, the anisotropy of the oriented film is high with front-face and in-line observations.

The anisotropy data for this model sensor are shown in Figure 10. The anisotropy decreases rapidly with increasing concentrations of Ru-HSA. It is important to notice that the sensitivity range of the assay can be adjusted by changing the concentration of Py2 in the PVA A lower concentration of Py2 results in a greater sensitivity to lower concentrations of Ru-HSA (---). For such assays it is not necessary to calculate the anisotropy. If desired, one can use the ratio of the polarized intensities. While the present measurements were performed with excitation of the bulk phase, one can also imagine situations where excitation is accomplished under conditions of total internal reflectance. internal reflectance fluorescence [TIRF] has been widely used for sensing and surface imaging [48-50]. Under these conditions the excited volume of the aqueous phase would penetrate into the solution only to a distance comparable to the wavelength.

EXAMPLE 6

All experiments were performed using sensors configured as shown in Figure 13. Excitation was with the 514 nm output of an air-cooled argon ion laser. The laser excitation was polarized 45° from the vertical. The emission was observed through an analyzer polarizer oriented parallel (||) or perpendicular (1) to the

20

25

30

35

laboratory vertical axis. When using an oriented film there is no need to use an excitation polarizer because the emission is highly polarized with polarized or unpolarized excitation. The polarization is given by

$$P = \frac{I_{l} - GI_{l}}{I_{l} + GI_{l}}$$

where I_{l} and I_{l} are the intensities observed with emission polarizer parallel or perpendicular to the polarized excitation, respectively. The G factor is the ratio of intensities (I_{l}/I_{l}) observed with horizontally polarized excitation [25]. In our apparatus the G-factor was near 1.0.

The oxygen sensor was prepared as described previously [51]. The ruthenium complex was synthesized in this laboratory. The silicone membrane was prepared by spreading a thin layer of GE Silicone II (Stock CE 5000, GE Silicones, General Electric Company, Waterford, NY) on a microscope slide using a blade. The thin layer (about 0.5 mm thick) was allowed to cure overnight and was then removed from the glass surface result in a in a thin transparent silicone membrane. The membrane was then soaked in a solution of the ruthenium complex in chloroform (typically 1.25 mg/mL) for 5 minutes allowing the silicone matrix to expand and absorb the fluorophore. The membrane was then removed and air dried for 5 minutes after which it shrank back to its original size. membrane was washed with ethanol to remove surface fluorophore molecules. In the final optrode configuration the membrane was positioned on the inner surface of the sensor cuvette.

Styryl 7 was obtained from Aldrich. Films of polyvinyl alcohol were prepared as described previously [22-23]. The method consists of dissolving the PVA in

10

20

25

30

35

water and polymerizing at ~360° K. Styryl 7 in methanol was added to a 10%-15% aqueous solution of polyvinyl alcohol. The PVA solution was then cast on a plate, and dried over a period of several days in a dust-free atmosphere. The PVA films were physically stretched at about 350°K up to 6-fold to orient the Styryl 7 molecules. The stretching ratio (R_s) is defined as the axial ratio a/b of an ellipse which is formed when stretching an imaginary circle in the unoriented film [23]. The volume of the circle or ellipse is assumed to be conserved. Under these conditions

$$R_s = N^{3/2}$$

15 where N is the physical fold of the stretch.

RESULTS

Oxygen Sensitive Film

Prior to describing polarization sensing of oxygen it is valuable to understand the properties of the samples and reference components. Emission spectra of $Ru(dpp)_3Cl_2$ in the silicon film are shown in Figure 23. The emission intensity is strongly dependent on the partial pressure of oxygen. An atmosphere of 100% oxygen results in an approximate 5-fold decrease in intensity.

The time response and reproducibility of the oxygen sensitive film were examined (Figure 24). The intensity changes rapidly and reproducibility as the atmosphere is changed respectively from air to nitrogen. Hence the oxygen-sensitive film responds reversibly and consistently under our experimental conditions.

Polarized Reference Film

It is also valuable to understand the spectral properties of the reference film. Emission spectra of

film, which is near 610 nm.

5

10

15

20

25

30

Styryl 7 in PVA are shown in Figure 25. Styryl 7 displays a good Stokes' shift, which results in minimal loss of polarization due to homo resonance energy transfer. The polarization is high in the PVA film because of the Styryl 7 molecules are immobile during the excited state lifetime in this viscous media. The polarization is mostly constant across the long wavelength absorption band and the emission spectrum, providing a high polarization at all useful wavelengths. The emission maximum of the reference film at 680 nm is considerably longer than that of the oxygen sensitive

While Styryl 7 in the unoriented film could be used as the reference, we chose to obtain a higher polarization using a stretched film. The effect of stretching on the steady state polarization is shown in Figure 26. A stretching ratio of $R_s = 12$ results in an anisotropy near 0.9 when using vertically polarized excitation. An important property of the stretched films is that they provide highly polarized emission even when excited with unpolarized light. This is shown in Figure 26 for the excitation polarization oriented at 45° from the vertical, which is equivalent to excitation with unpolarized light. Prior to stretching the anisotropy values with 45° excitation are one-half of that found using a vertically polarized light, which is the result expected from the theory for photoselection [25]. As the film is stretched the polarization with unpolarized excitation increases rapidly, and approaches the values found with polarized excitation (Figure 26). This occurs because the electronic transitions are oriented along the stretch axis. The orientation provides the same effect as the polarizer, to orient the emission dipoles vertically in the laboratory axis.

5

10

15

20

25

30

35



Oxygen Sensor

The oxygen sensor contains both $Ru(dpp)_3Cl_2$ and Styryl 7. Emission spectra from the combined oxygen sensor (Figure 13) are shown in Figure 14 (top). When the analyzer polarizer is in the vertical position, the emission spectrum seen through the analyzer is equivalent to that of the Styryl 7-PVA film (____). This is because the horizontally polarizer emission from $Ru(dpp)_3Cl_2$ is eliminated by the analyzer polarizer.

Emission spectra from the sensor were also recorded with the analyzer in the horizontal position (Figure 14, ---). In this case there is observable emission from both $Ru(dpp)_3Cl_2$ and Styryl 7. There is a contribution from Styryl 7 because the molecules are not perfectly aligned, so there is a significant horizontal component.

Because of the spectral shift between $Ru(dpp)_3Cl_2$ and Styryl 7 the relative emission from each will depend on the observation wavelength. We measured the polarization across the emission spectra (Figure 14, bottom). The polarization increases with increasing wavelength because Styryl 7 emits at longer wavelengths than $Ru(dpp)_3Cl_2$. Hence, the vertically polarized emission of Styryl 7 becomes dominant at longer wavelengths. The polarization values at most observation wavelengths were found to increase with increasing oxygen concentrations (Figure 14, bottom). This occurs because oxygen quenches the emission of $Ru(dpp)_3Cl_2$, and does not affect the emission from Styryl 7.

The oxygen-dependent polarization values were used to develop a calibration curve for oxygen (Figure 15). The polarization increases due to quenching of the horizontally polarized emission from $Ru(dpp)_3Cl_2$. Importantly, the polarization values display large changes, from -0.33 to +0.45 for the range from 0 to 100% oxygen. Since polarization values are routinely

determined to better than ± 0.01 , one can expect accuracy in the oxygen concentration of 1% or better.

EXAMPLE 7

HSA and ANS were obtained from Sigma, Inc. and used without further purification. The HSA concentration was 3.3 mg/ml. The ANS concentration was $1.2 \times 10^{-5} \,\mathrm{M}$ as calculated from ϵ (372 nm) = 7,800 M⁻¹ cm⁻¹. The solution of HSA and ANS was in 0.05 M phosphate buffer, pH = 7.

The glucose assay was accomplished using the glucose/galactose binding protein from *E. Coli* (GGBP). We used a mutant which contained a single cysteine residue at position 26 (Q26C GGBP) [15]. This protein was labeled with

- (4'iodoacetamidoanilino)naphthalene-6-sulfonic acid
 (I-ANS) from Molecular Probes, Inc. A solution
 containing 2.5 mg/ml Q26C GGBP in 20 mM phosphate, 1 mM
 tris-(2-carboxyethy)phosphine (TCEP), pH 7.0 was reacted
 with 50 μL of a 20 mM solution of I-ANS in
- tetrahydrofuran (purchased from Molecular Probes, Inc.).

 The resulting labeled protein was separated from the free dye by passing the solution through a Sephadex G-25 column. The protein-ANS conjugate was purified further on Sephadex G-100 and dissolved in 20 mM phosphate, pH

 7.0.

Fluo-3 was obtained from Molecular Probes, Inc. The calcium concentration was controlled using the calcium buffer kits, C-3009, also from Molecular Probes, Inc.

30 **RESULTS**

35

Operating Principle of Self-Referenced Polarization Sensing

To illustrate the principles of polarization sensing we chose to initially present our results using two different fluorophores. One side (V) of the sensor

5

10

15

20

25

30

35

contained a constant concentration of HSA with non-covalently bound ANS. The other side (H) of the sensor contained the glucose/galactose binding protein from *E. Coli*. These samples displayed similar but slightly different emission spectra. The emission maxima for ANS/HSA and ANS-Q26C GGBP were 485 and 450 nm, respectively.

The different emission maxima for the two sides of the sensor allows visualization for the contribution from each fluorophore to the total emission. The emission spectra were recorded from the combined sensor (Figure 16). When the emission polarizer was in the vertical orientation the emission spectra was characteristic of ANS/HSA. When the emission polarizer is in the horizontal position the emission spectrum was characteristic of labeled GGBP. The emission spectra observed through a vertically or horizontally oriented polarizer represent the emission from ANS/HSA and ANS-Q26C GGBP, respectively.

GGBP labeled with I-ANS displays only a moderate change in intensity due to glucose. From other experiments we know that the glucose binding constant is near 1 μ M [15]. Addition of 8 μ M glucose to labeled GGBP results in an approximate two-fold decrease in the intensity of the ANS label (Figure 16). We used this decrease as the basis of our polarization sensor.

Polarization values were measured across the emission spectra from the combined sensor (Figure 17). The polarization values increase with increasing wavelength. This effect is due to the increasing contribution of ANS/HSA at longer wavelengths, and the vertically oriented polarizer in front of ANS/HSA. The polarization values are lower and even negative at shorter wavelengths because of the shorter wavelength emission of ANS-Q26C GGBP and the horizontal polarizer in

10

15

20



front of this sample. The polarization values were also found to be dependent on the glucose concentration. Increasing amounts of glucose result in larger polarization values. This change occurs because binding of glucose to labeled GGBP decreases its intensity. Hence the polarization shifts towards the value of +1.0 characteristic of the ANS/HSA side of the sensor.

We used the glucose-dependent polarization values to develop a calibration curve for glucose (Figure 18). It is surprising to notice that the polarization increases substantially from 0.06 to 0.36. This range is larger than encountered for typical polarization assays in which the polarization change is due to changes in the rotational correlation time of the fluorophore. This larger range of polarization values is the result of using a pair of orthogonally oriented polarizers as part of the sensor design. The increase in polarization is complete above 6 $\mu\rm M$ glucose. This occurs because ANSQ26C GGBP becomes saturated with glucose and the intensity becomes constant.

It is informative to consider the potential accuracy of these glucose measurements. Since polarization measurements are easily accurate to ± 0.01 , we estimate the accuracy in glucose concentrations to be about ±0.1 In the future one can expect glucose binding 25 proteins which display larger changes in intensity than ANS-Q26C GGBP. In these cases the polarization change will be larger, and the accuracy in the glucose concentration will be higher. Of course the maximum 30 accuracy will be found near the midpoint of the glucose-GGBP binding curve. The accuracy will decrease as the glucose concentration becomes much smaller or much larger than the glucose binding constant.

5

10

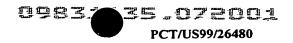
15

. 20

25

30

35



EXAMPLE 8

We next examined a sensor which contained ANS-Q26C GGBP on both sides of the sensor. The reference solution was observed through a vertical polarizer, and the solution with various glucose concentrations was observed through a horizontal polarizer (Figure 19, top). the analyzed polarizer was in the vertical orientation, the emission spectrum was independent of glucose concentration (___). This occurs because the vertical analyzer polarizer selects for emission from the reference side of the sensor. When the analyzer polarizer is in the horizontal orientation the emission spectra display decreasing intensity with increasing glucose concentration (---). This occurs because the horizontal analyzer selects from the emission from the side of the sensor which contains the variable glucose concentration.

We measured the polarization spectra for the combined emission from the sensor (Figure 19, bottom). In this case the polarization values are independent of wavelength because both sides of the sensor display the same emission spectra. This is an advantage of using the sensor as the reference, as there is no dependence of the polarization values on the observation wavelength. As the glucose concentration increases the polarization increases. This increase occurs because the intensity ANS labeled GGBP decreases in the presence of glucose, so that the vertically polarized reference emission contributes a larger fraction to the total emission.

The polarization values were again used to develop a glucose calibration curve (Figure 20). In this case the polarization changes from near zero to over 0.3. This change in polarization occurs for only a two-fold change in sample intensity. Since the reference and sample are the same fluorophore, one expects both sides of the

10

15

20

25

30

35

sensor to display similar photobleaching or dependence on temperature. Hence the glucose calibration curve should be stable for extended periods of time.

One may question the usefulness of a glucose sensor with micromolar sensitivity when the concentration of glucose in the blood is near 5 mM. High glucose affinity is useful for two reasons. First, one can use a minimum volume of blood which is then diluted into the sample in contact with the sensor. Secondly, there is increasing interest in the use of extracted interstitial fluid to monitor blood glucose. In this sample the glucose concentration is often in the micromolar range [52].

EXAMPLE 9

Fluorescence sensing methods are needed for a variety of cations and anions, particularly for blood gases and electrolytes. Hence we examined how our polarization sensor could be used to measure calcium. For these experiments we chose the calcium-sensitive fluorophore Fluo-3 [53]. This fluorophore displays a dramatic increase in fluorescence upon binding calcium, approximately 100-fold [30]. While the intensity change of Fluo-3 is dramatic, there is no spectral shift upon calcium binding. Hence, wavelength-ratiometric measurements are not possible. Furthermore, Fluo-3 is not useful with lifetime-based sensing. This is because Fluo-3 is non-fluorescent in the absence of calcium. the lifetime is measured, one only observes the emission from the calcium-bound form. Hence, the lifetimes are independent of calcium concentration.

While Fluo-3 is not useful as a wavelength-ratiometric of lifetime sensor, its large change in intensity makes it well suited for use in polarization sensing. The sensor was configured with Fluo-3 in both sides. The calcium concentration was constant at 1.35 $\mu\rm M$ in the

5

10

15

20

reference (vertical) side, and was variable in the sample (horizontal) side of the sensor. Emission spectra were recorded through the analyzer polarizer (Figure 21, top). The spectrum was constant with the analyzer in the vertical orientation because of the constant signal from the vertical side of the sensor. The emission spectrum seen with the analyzer in the horizontal position increases with the calcium concentration because of the intensity increase of Fluo-3.

Since the sensor contained Fluo-3 on both sides, the polarization was independent of wavelength (Figure 21, The polarization decreased dramatically from 0.8 to 0.0 with increasing calcium concentrations. decrease in polarization occurs because the intensity from the horizontally polarized side of the sensor increases as the calcium concentration increases. The calibration curve for the polarization values (Figure 22) shows a dramatic dependence on the calcium concentration. In this case the calcium concentrations are expected to be accurate to $\pm 0.01~\mu\mathrm{M}$. Once again, since the same fluorophore is present on both sides of the sensor, one expects similar changes in the emission due to temperature or photobleaching. Hence one can anticipate a stable calcium calibration curve. If desired, the polarization could increase with higher calcium concentrations by reversing the sample and reference in Scheme I. The calcium-sensitive range is from 0 to 400 nM Ca²⁺, which is the typical range for intracellular calcium.

30

25

REFERENCES

- Wolfbeis, O. S., Ed. (1991). Fiber Optic Chemical Sensors and Biosensors, Volume I, CRC Press, Boca
 Raton, pp. 413.
 - Wolfbeis, O. S., Ed. (1991). Fiber Optic Chemical Sensors and Biosensors, Volume II, CRC Press, Boca Raton, pp. 358.

10

25

- 3. Spichiger-Keller, U. E. (1998). Chemical Sensors and Biosensors for Medical and Biological Applications, Wiley-VCH, New York, pp. 413.
- 15 4. Schulman, S. G., Ed. (1993). Molecular Luminescence Spectroscopy, Methods and Applications: Part 3, John Wiley & Sons, Inc., New York, pp. 467.
- 5. Lakowicz, J. R., Ed. (1994). Topics in Fluorescence

 Spectroscopy, Volume 4: Probe Design and Chemical

 Sensing, Plenum Press, New York, pp. 501.
 - 6. Kunz, R. E., Ed. (1997). Proc. of 3rd European Conference on Optical Chemical Sensors and Biosensors, Europt(R)odeIII. Sensors and Actuators B, Elsevier Publishers, New York, B38, pp1-188, and B39, pp1-468.
- 7. Thompson, R. B. (Ed.) (1997). Advances in

 Fluorescence Sensing Technology III, SPIE Proc.,

 Volume 2980, pp. 582.
 - 8. Lippitsch, M. E., Draxler, S., and Kieslinger, D. (1997). Luminescence lifetime-based sensing: new

materials, new devices, Sensors and Actuators B 38-39:96-102.

- 9. Lippitsch, M. E., Pusterhofer, J., Leiner, M. J. P., and Wolfbeis, O. S. (1988). Fibre-optic oxygen sensor with the fluorescence decay time as the information carrier, *Anal. Chim. Acta* 205:1-6.
- Szmacinski, H., and Lakowicz, J. R. (1994).
 "Lifetime-based sensing," in Topics in Fluorescence Spectroscopy: Vol. 4: Probe Design and Chemical Sensing (J. R. Lakowicz, Ed.), Plenum Press, New York, pp. 295-334.
- 15 11. Terpetschnig, E., Szmacinski, H., and Lakowicz, J. R. (1997). Long-lifetime metal-ligand complexes as probes in biophysics and clinical chemistry, *Methods in Enzymology*, Academic Press, pp. 295-321.
- 20 12. Szmacinski, H., Castellano, F. N., Terpetschnig, E., Dattelbaum, J. D., Lakowicz, J. R., and Meyer, G. J. (1997). Long-lifetime Ru(II) complexes for the measurement of high molecular weight protein hydrodynamics, Biochim. et. Biophys. Acta 1383:151-159.
 - 13. Neurauter, G., Klimant, I., Liebsch, G., Kosch, U., and Wolfbeis, O. S. (1998). A comparative study on different types of intensity independent optical pCO₂ sensors, *Europt(r) ode IV*, German Chemical Society, pp. 231-232.
 - 14. Klimant, I., and Wolfbeis, O. S. (1998). Dual luminophore referenced optodes: A convenient way to

15

25



convert the fluorescence intensity into a phase shift or time dependent parameter, *Europt(r)ode IV*, German Chemical Society, pp. 125-126.

- 5 15. Tolosa, L., Gryczynski, I., Eichhorn, L.,
 Dattelbaum, J. D., Castellano, F. N., Rao, G., and
 Lakowicz, J. R. (1998). Glucose sensor for low cost
 lifetime-based sensing using a genetically
 engineered protein, Anal. Biochem. submitted.
- 16. Lakowicz, J. R., Castellano, F. N., Dattelbaum, J. D., Tolosa, L., Rao, G., and Gryczynski, I. (1998). Low frequency modulation sensors using nanosecond fluorophores, Anal. Chem., submitted.
- 17. Lakowicz, J. R., Dattelbaum, J. D., and Gryczynski, I. (1998). Quantitative intensity measurements in scattering media, Sensors and Actuators, submitted.
- 20 18. Jabłoński, A. (1960). On the notion of emission anisotropy, Bull. Acad. Pol. Sci. 8:259-264.
 - 19. Sacksteder, L. A., Lee, M., Demas, J. N., and DeGraff, B. A. (1993). Long-lived, highly luminescent rhenium(I) complexes as molecular probes: intra- and intermolecular excited-state interactions, J. Am. Chem. Soc. 115:8230-8238.
- 20. Juris, A., and Balzani, V. (1988). Ru(II)
 30 polypyridine complexes: photophysics,
 photochemistry, electrochemistry and
 chemiluminescence, Coord. Chem. Rev. 84:85-277.
 - 21. Michl, J., and Thulstrup, E. W. (1986). Spectroscopy

With Polarized Light, VCH Publishers, New York, pp. 573.

- 22. Kawski, A., and Gryczynski, Z. (1987). On the determination of transition-moment directions from absorption anisotropy measurements, Z. Naturforsch. 42a:617-621.
- 23. Kawski, A., Gryczynski, Z., Gryczynski, I., Lakowicz, J. R., and Piszczek, G. (1996). Photoselection of luminescent molecules in anisotropic media in the case of two-photon excitation. Part II. Experimental studies of Hoechst 33342 in stretched poly(vinyl alcohol) films, Z. Naturforsch. 51a:1037-1041.
- 24. Sipior, J., Carter, G. M., Lakowicz, J. R., and Rao, G. (1996). Single quantum well light emitting diodes demonstrating as excitation sources for nanosecond phase-modulation fluorescence lifetime measurements, Rev. Sci. Instrum. 67(11):3795-3798.
- 25. Lakowicz, J. R. (1999). Principles of Fluorescence Spectroscopy, 2nd Edition, Plenum Publishing Co.,
 New York, in press.

30

- 26. Castellano, F. N., Dattelbaum, F. N., and Lakowicz, J. R. (1998). Long-lifetime Ru(II) complexes as labeling reagents for sulfhydryl groups, Anal. Biochem. 255:165-170.
- 27. Matczuk, A., Bojarski, P., Gryczynski, I., Kuśba, J., Kulak, L., and Bojarski, C. (1995). The influence of water structure on the rotational

depolarization of fluorescence, *J. Photochem.*Photobiol. A. **90**:91-94.

- 28. Babcock, D. F. (1983). Examination of the intracellular ionic environment and of ionophore action by null point measurements employing the fluorescein chromophore, *J. Biol. Chem.* 258:6380-6389.
- 10 29. Klonis, N., Clayton, A. H. A., Voss, E. W., and Sawyer, W. H. (1998). Spectral properties of fluorescein in solvent-water mixtures: Applications as a probe of hydrogen bonding environments in biological systems, *Photochem. Photobiol*. 67:500-510.
 - 30. Molecular Probes Catalogue (1996). Sixth Edition, Richard P. Haugland, Ed., pp. 551-561.
- 31. Mahutte, C. K., Holody, M., Maxwell, T. P., Chen, P. A., and Sasse, S. A. (1994). Development of a patient-dedicated, on-demand, blood gas monitor, Am. J. Respir. Crit. Care Med. 149:852-859.
- 25 32. Mahutte, C. K., Sasse, S. A., Chen, P. A., and Holody, M. (1994). Performance of a patient-dedicated, on-demand blood gas monitor in medical ICU patients, Am. J. Respir. Crit. Care Med. 150:865-869.
 - 33. Mahutte, C. K. (1994). Continuous intra-arterial blood gas monitoring, *Intensive Care Med.* **20:**85-86.
 - 34. Tsien, R. Y. (1989). Fluorescent indicators of ion

concentrations in *Methods in Cell Biology*, Academic Press, New York, pp. 127-156.

- 35. Kao, J. P. Y. (1994). Practical aspects of measuring [Ca²⁺] with fluorescent indicators in *Methods in Cell Biology*, Academic Press, New York, **40**:155-181.
- 36. Lakowicz, J. R., Szmacinski, H., and Johnson, M. L. (1992). Calcium concentration imaging using
 fluorescence lifetime and long-wavelength probes, J. Fluoresc. 2(1):47-62.
- 37. Lakowicz, J. R., and Szmacinski, H. (1992).

 Fluorescence lifetime-based sensing of pH, Ca²⁺, K⁺
 and glucose, Sensors and Actuators B **11**:133-143.
- 38. Kao, J. P. Y., Harootunian, A. T., and Tsien, R. Y. (1989). Photochemically generated cytosolic calcium pulses and their detection by Fluo-3, *J. Biol. Chem.* 20 264:8179-8184.
- Valeur, B. (1994). "Principles of fluorescent probe design for ion recognition," in Topics in Fluorescence Spectroscopy, Vol. 4: Probe Design and Chemical Sensing (J. R. Lakowicz, Ed.), Plenum Press, New York, pp. 21-48.
- 40. Czarnik, A. W. (1994). "Fluorescent chemosensors for cations, anions, and neutral analytes," in *Topics in Fluorescence Spectroscopy*, Vol. 4: Probe Design and Chemical Sensing (J. R. Lakowicz, Ed.), Plenum Press, New York, pp. 49-70.
 - 41. Verkman, A. S., Sellers, M. C., Chao, A. C. Leung,

T., and Ketcham, R. (1989). Synthesis and characterization of improved chloride-sensitive fluorescent indicators for biological applications, *Anal. Biochem.* **178**:355-361.

5

- 42. Biwersi, J., Tulk, B., and Verkman, A. S. (1994). Long-wavelength chloride-sensitive fluorescent indicators, *Anal. Biochem.* **219**:139-143.
- 10 43. Bacon, J. R., and Demas, J. N. (1987). Determination of oxygen concentrations by luminescence quenching of a polymer immobilized transition metal complex,

 Anal. Chem. 59:2780-2785.
- 15 44. Carraway, E. R., Demas, J. N., DeGraff, B. A., and Bacon, J. R. (1991). Photophysics and photochemistry of oxygen sensors based on luminescent transition-metal complexes, *Anal. Chem.* **63**:337-342.
- 20 45. Van Dyke, K., and Van Dyke, R., Eds. (1990).

 Luminescence Immunoassay and Molecular Applications,
 CRC Press, Boca Raton, pp. 341.
- 46. Guo, X-Q., Castellano, F. N., Li, L., and Lakowicz, J. R. (1998). Use of a long-lifetime Re(I) complex in fluorescence polarization immunoassays of highmolecular weight analytes, Anal. Chem. 70(3):632-637.
- 30 47. Guo, X-G., Castellano, F. N., Li, L., Szmacinski, H., Lakowicz, J. R., and Sipior, J. (1997). A long-lived highly luminescent Re(I) metal-ligand complex as a biomolecular probe, Anal. Biochem. 254:179-186.



48. Axelrod, D., Hellen, E. H., and Fulbright, R. M. (1992). "Total internal reflection fluorescence," in Topics in Fluorescence Spectroscopy, Vol. 3: Biochemical Applications, Plenum Press, New York, pp. 289-343.

5

10

25

- 49. Zhou, Y., Laybourn, P. J. R., Magill, J. V., and De La Rue, R. M. (1991). An evanescent fluorescence biosensor using ion-exchanged buried waveguides and the enhancement of peak fluorescence, *Biosensors & Bioelectronics* 6:595-607.
- 50. Olveczky, B. P., Periasamy, N., and Verkman, A. S. (1997). Mapping fluorophore distributions in three dimensions by quantitative multiple angle-total internal reflectance fluorescence microscopy, Biophys. J. 73:2836-2847.
- 51. Bambot, S.B., et al., (1994). Phase fluorometric 20 sterilizable optical oxygen sensor, Biotech. Bioeng. 43:1139-1145.
 - 52. Tamada, J.A., et al., Nature Medicine, 2(11), 1198-1201.
 - 53. Minta, A., et al., J. Biol. Chem., **264(14)**, 8171-8178 (1989).

5

10

20

30



CLAIMS

- A method for determining the presence or concentration of an analyte, comprising the steps of:
- a) exposing a fluorescent reference molecule and a fluorescent sensing molecule to a radiation source;
- b) measuring a first level of anisotropy of the combined fluorescence emitted by said molecules;
- c) exposing said sensing molecule to an analyte, wherein said analyte is capable of changing the intensity of the fluorescence emitted by the sensing molecule;
- d) measuring a second level of anisotropy of the combined fluorescence emitted by said molecules after exposure of the sensing molecule to said analyte; and
- e) correlating a change in said second level of
 anisotropy with the presence or concentration of said analyte.
 - 2. The method of claim 1, wherein the fluorescent reference molecule is a long-lifetime metal-ligand complex.
 - 3. The method of claim 1, wherein the fluorescent reference molecule displays an anisotropy near zero.
- 4. The method of claim 1, wherein the fluorescent reference molecule displays an anisotropy near one.
 - 5. The method of claim 4, wherein the fluorescent reference molecule is embedded in a film.
 - 6. The method of claim 5, wherein the film is a stretched polymer film.
- 7. The method of claim 1, wherein the analyte is selected from the group consisting of an ion, oxygen,

protein, lipoprotein, glycoprotein, peptide, nucleic acid, polysaccharide, lipopolysaccharide, lipid, fatty acid, cellular metabolite, hormone, pharmacological agent, antibody, and a sugar.

5

8. The method of claim 1, wherein the method determines pH.

9. The method of claim 8, wherein the fluorescent sensing molecule is a pH sensitive fluorescein.

- 10. The method of claim 9, wherein the fluorescent reference molecule is pyridine 2 in a stretched film.
- 11. The method of claim 1, wherein the reference and sensing molecules are distinct molecules having the same structure, and wherein the reference molecule is not exposed to the analyte.
- 20 12. The method of claim 1, wherein the reference molecule is exposed to the analyte only if such exposure is not capable of changing the intensity of the fluorescence emitted by the reference molecule.
- 25 13. A device for determining the presence or concentration of an analyte, which comprises:
 - a) means for exposing a fluorescent reference molecule and a fluorescent sensing molecule to a radiation source;
- 30 b) means for measuring the anisotropy of the combined fluorescence emitted by said molecules;
 - c) means for exposing said sensing molecule to an analyte;
- d) optionally means for correlating a change in
 35 said level of anisotropy from before to after exposure to





the analyte with the presence or concentration of said analyte; and

- e) optionally a radiation source capable of causing said reference and sensing molecules to emit fluorescence.
- 14. The sensor of claim 13, which additionally comprises a polarizer whose emission is perpendicular to that of the reference molecule.